PROCEEDINGS OF SCIENCE

Two-particle correlations in p-p and Pb-Pb collisions with the ATLAS detector at the LHC

Regina Kwee for the ATLAS Collaboration*
CERN/Humboldt University of Berlin
E-mail: Regina.Kwee@cern.ch

An overview of two angular correlation analyses with the ATLAS detector at the LHC is presented. Two-particle correlations are measured in proton-proton collisions at two centre-of-mass energies, $\sqrt{s} = 0.9$ and 7 TeV, recorded at the beginng of LHC beam operation in 2009 and 2010. A kinematic range is defined for these measurements considering primary charged particles with a transverse momentum of $p_T > 100$ MeV and a pseudorapidity of $|\eta| < 2.5$. The results are corrected for detector effects and compared to several Monte-Carlo models including tunes of PYTHIA6, PYTHIA8 and PHOJET. In lead-lead collisions, particle correlations are analysed by measuring flow components of the azimuthal angular distribution. Measurements of the "medium", created in such ultra-relativistic heavy ion collisions at $\sqrt{s_{NN}} = 2.76$ TeV as in 2010, provide significant constraints for modeling its dynamical evolution. The results of the analysis of the v_2-component, also known as *ellliptic flow*, cover a p_T-range from $p_T = 0.5$ to 20 GeV and as well $|\eta| < 2.5$. Higher order flow components are also presented.

The Seventh Workshop on Particle Correlations and Femtoscopy
September 20 - 24 2011
University of Tokyo, Japan

*Speaker.

ATL-PHYS-PROC-2012-050
22 March 2012

PoS(WPCF2011)022

1. Introduction

The study of particle correlations at high energies provide information on several aspects of the underlying processes: the initial dynamics of the particles and the asymmetric energy deposition during hadron collisions are tranferred to final state particles manifesting themselves in angular correlations. This allows to investigate the underlying mechanism of soft particle production, fragmentation and jet formation. Of particular interest is the study of a new medium, the Quark-Gluon-Plasma (QGP) [1], an extremely dense and hot matter state that is created in ultrarelativistic heavy ion collisions. Measurements of flow components of this matter state probe various hydrodynamic models that are used to describe QGP. In particular, the study of primary charged particle correlations in proton-proton (pp) enable disentanglement of single- and multi-hadron behaviour when compared to corresponding correlation studies in lead-lead (Pb-Pb) collisions. Two such studies are presented with the ATLAS experiment.

2. The ATLAS Detector and Trigger System

ATLAS is one of the two general purpose experiments at the Large Hadron Collider (LHC) at CERN. Two main sub-systems of the ATLAS detector [2] were used for the anayses: the Inner Detector (ID) for measurements of primary charged particles and the forward calorimetry system (FCal) for measurements of the energy created event-by-event basis. The ID coveres a pseudorapidity[1] region of $|\eta| < 2.5$ and has two high-precision trackers made of silicon pixels (Pixel) in the innermost detector part of ATLAS and semiconducting microstrip trackers (SCT) surrounding them. The angular resolution in azimuth (denoted as ϕ) ranges from 40 to 50 μrad at $\eta \simeq 0.25$ and $\eta \simeq 1.75$, respectively, and from 5 to 10 in $\cot\theta$. A charged particle typically hits the ID in three layers of the Pixel and four layers of the SCT detector before passing through the transition radiation tracker (TRT) that is composed of drift tubes. The FCal covers a pseudorapidity range from $3.2 < |\eta| < 4.9$ and uses tungsten and copper as absorber material and liquid argon as active medium comprising in total about 10 interaction lengths.

The ATLAS trigger system is a three-level trigger with hardware triggers at Level-1 (L1) and software triggers at Level-2 (L2) and at the third level, the Event Filter (EF). Inelastic interactions were selected with the Minimum Bias Trigger Scintillators (MBTS) at L1. The MBTS are located at ± 3.56 m away from the interaction point (IP) and consist of 16 scintillator counters per side covering $2.09 < |\eta| < 3.89$. For the pp analysis, at least one of the counters must have fired. For the Pb-Pb analysis, a coincidence of signals were required either in the MBTS or in the Zero-Degree-Calorimeter (ZDC) which is positioned a ± 140 m from the IP detecting neutrons and photons with $|\eta| > 8.3$. While coincidence of hits in the ZDC was sufficient to select the event, the coincidence of MBTS hits is followed by a further selection step at L2 where timing information is used to suppress beam-background events.

For the pp-analysis, data of 7 μb^{-1} were recorded in 2009 at a centre-of-mass energy of $\sqrt{s} = 0.9$ TeV and 190 μb^{-1} in 2010 at $\sqrt{s} = 7$ TeV, whereas approximately 7 μb^{-1} of Pb-Pb collisions were recorded in 2010 at an nucleus-nucleus energy of $\sqrt{s_{NN}} = 2.76$ TeV.

[1] Pseudorapidity η is defined as $\eta = -\ln\tan\theta/2$ with θ the polar angle measured w.r.t. to the beam-axis.

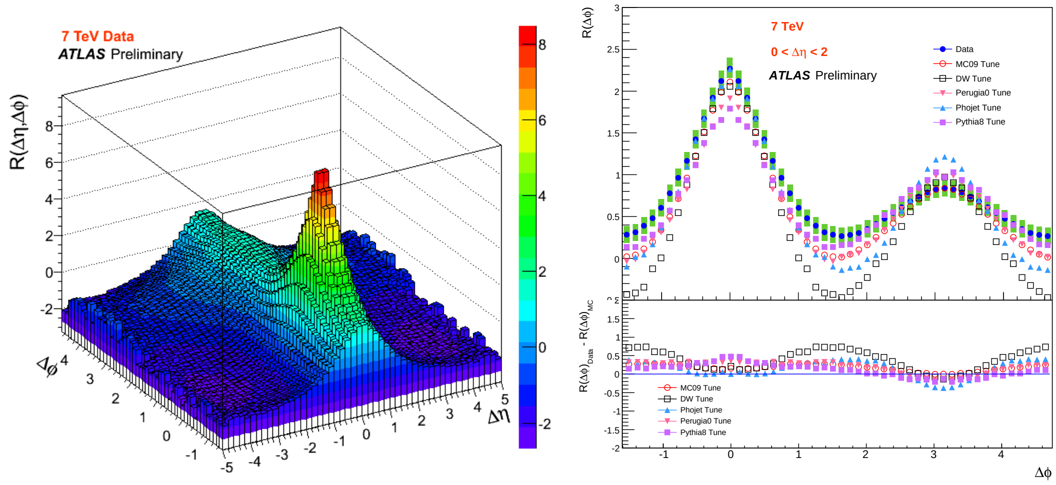

(a) (b)

Figure 1: Two-particle correlations at $\sqrt{s} = 7$ TeV after correcting for trigger, detector and reconstruction effects. (a) shows the 2-dimensional correlation function R($\Delta\eta$, $\Delta\phi$), (b) shows azimuthal correlation function R($\Delta\phi$) integrated over $0 < \Delta\eta < 2$ comparing to predictions of several Monte-Carlo models with the absolute difference in the bottom insert. See also Ref. [3].

3. Analysis of two-particle correlations in proton-proton collisions

The observable to study two-particle correlations in pp-collisions is formed by dividing two selected samples, the foreground sample F, consisting of correlated and uncorrelated $\Delta\phi$ and $\Delta\eta$ pairs of primary charged particles within one event, and the background sample B, consisting of uncorrelated $\Delta\phi$ and $\Delta\eta$ pairs formed from different events, as detailed in Ref. [4]. This formally gives the two-particle correlation function

$$R(\Delta\phi,\Delta\eta) = \frac{\langle (n_{\rm ch}-1)\,F(n_{\rm ch},\Delta\phi,\Delta\eta)\rangle_{ch}}{B(\Delta\phi,\Delta\eta)} - \langle n_{\rm ch}-1\rangle_{ch} \tag{3.1}$$

where $\langle \ldots \rangle_{ch}$ denotes an average over the number of charged particles $n_{\rm ch}$ in the event.

The analysis is performed within a phase-space region defined by kinematic cuts of the selected tracks requiring a transverse momentum of $p_T > 100$ MeV and $|\eta| < 2.5$. The track selection consists of applying certain track quality cuts [4] to ensure that tracks of well reconstructed primary charged particles are counted. A correction procedure is applied to the data to unfold for detector and reconstruction effects in a data-driven manner. Therfore, events are first weighted on an event-by-event basis accounting for trigger and vertex reconstruction inefficiencies. In a second step, the observable is computed according to Eq. 3.1 and data are corrected using a new, model-indepent, so-called *Hit Backspace Once More (HBOM)* method [5]. In this method, the detector effects are iteratively applied to the data. At each iteration step, each bin-value of the observable is fitted to a polynominal function and extrapolated backwards in order to obtain the bin-value of the observable before detector effects were present. The detector effects are at each iteration step applied by removal of single tracks, if a random number, generated for each track, is greater than the single track reconstruction efficiency. The iterations are repeatedly performed as long as the statistics of the dataset allow.

3.1 Results

The results of the corrected two-particle correlation functions are shown for data at $\sqrt{s} = 7$ TeV in Fig. 1. One can observe several contributions to the structure of the 2-dimensional correlation function as depicted in Fig. 1 (a). At $(\Delta\phi, \Delta\eta) \approx (0{,}0)$, particles are emitted closely related to each other having a relative high p_T and forming the narrow peak. The ridge at $\Delta\phi \approx \pi$ extending along all $\Delta\eta$ contains contributions due to momentum conservation leading to particles being produced back-to-back. A further structure can be recognised at $\Delta\eta \approx 0$ which can be associated to decay of lower p_T particles such as decay of resonances. The short-range correlations (integrated over $0 < \Delta\eta < 2$) are shown in Fig. 1 (b). The comparison of the data with several PYTHIA6 Monte Carlo models (MC09, DW, PERUGIA0) and two different soft QCD models employed in PHOJET and PYTHIA8 (for details see Ref. [3]) exhibit clear differences with the data, only the strength of the correlation at around $\Delta\phi = 0$ seems to be underestimated by all models. The two-particle correlations were also measured at $\sqrt{s} = 0.9$ TeV. At lower centre-of-mass energy, the peak at $(\Delta\phi, \Delta\eta)$ $\approx (0{,}0)$ is smaller, however the away-side correlations (integration over $\pi/2 < \Delta\phi < \pi$) exhibit a constant strength, further details can be found in Ref. [3]. Moreover, the analyis as presented in this reference has been extended in Ref. [4] by an analysis of another phase-space region requiring $n_{\mathrm{ch}} \geq 20$.

4. Anisotropic flow measurements in lead-lead collisions

Anisotropic flow is sensitive to initial asymmetries in the geometry of the colliding system, a consequence of spatial asymmetries which develop only in the first fm [6]. Collective flow measurements in heavy-ion collisions provide thus direct access to the early stage of the evolution of the system. They are modeled by relativistic models of hydrodynamics.

The analyis of anisotropic flow is usually performed by decomposing the azimuthal angular distribution of final state particles in Fourier series according to Eq. 4.1 with ϕ the azimuthal angle, v_n and $\Psi_{RP,n}$ the magnitude and the azimuth angle of the n^{th}-order reaction plane, respectively.

$$E\frac{d^3N}{dp^3} = \frac{1}{p_T}\frac{d^3N}{d\phi\, dp_T\, dy} = \frac{1}{2\pi p_T}\frac{E}{p}\frac{d^2N}{dp_T\, d\eta}\left(1 + 2\sum_{n=1}^{\infty} v_n(p_T)\cos[n(\phi - \Psi_{RP,n})]\right) \tag{4.1}$$

Measurements of the Fourier coefficients v_n, generally defined as $v_n = \langle\cos[n(\phi - \Psi_{RP,n})]\rangle$, quantify the anisotropic flow and provide constraints on relativistic hydrodynamic models. To systematically select various geometries of intial states, the flow components are measured in bins of *centrality*. They are determined by total amount of transverse energy, $\sum E_T$, deposited in the forward calorimeter. Events with the largest $\sum E_T$ correspond to the most central collisions arising from inelastic, non-coulomb interactions, entering in the first centrality bin starting at 0 %. The most peripheral collisions are attributed to the highest centrality bin which goes up to 100 %. In Ref [7], p_T and η-spectra of the second coefficient v_2, also named *elliptic flow*, are measured in bins of centrality in the pseudorapidity region $|\eta| < 2.5$ over the full azimuthal range $0 < \phi < 2\pi$ and for transverse momenta of $0.5 < p_T < 20$ GeV. In this analysis [7], the reaction plane was approximated by the event plane

$$\Psi_{RP,2} \approx \Psi_2 = \frac{1}{2}\tan^{-1}\left(\frac{\sum_i E_{T,i} w_i \sin(2\phi_i)}{\sum_i E_{T,i} w_i \cos(2\phi_i)}\right) \tag{4.2}$$

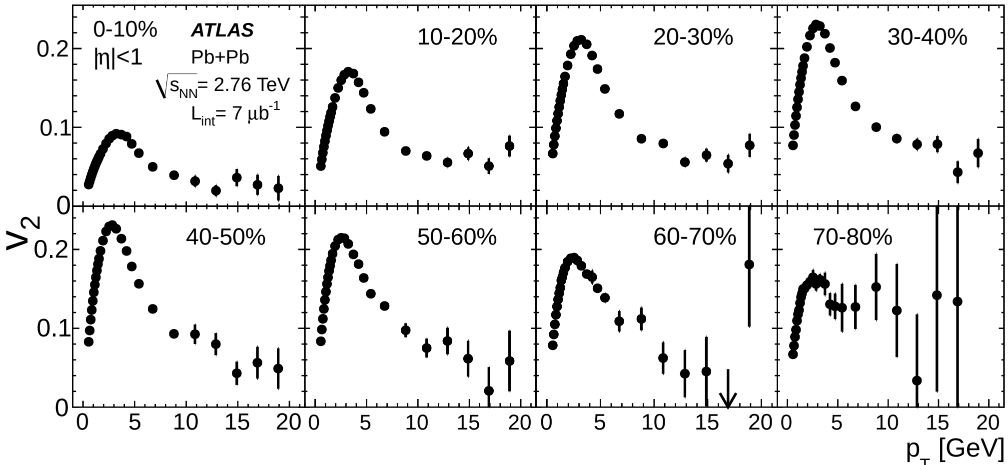

Figure 2: Dependence of elliptic flow v_2 of centrality and p_T for correlations with $|\eta| < 1$. Similar trends are measured at larger pseudorapidities, see Ref. [7].

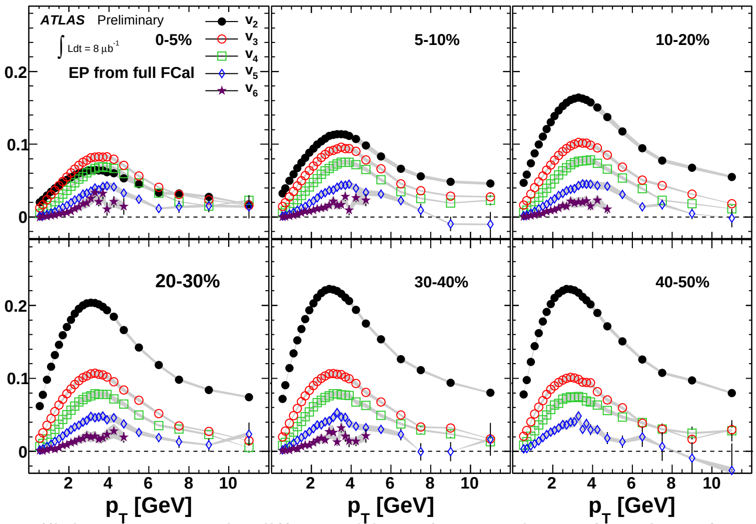

Figure 3: Flow coefficients v_2 to v_6 in different bins of centrality as function of p_T from Ref. [8].

with the sums going over each *tower* i in which the transverse energy $E_{T,i}$ of the first sampling layers of the forward calorimeter is measured, w_i are tower weights to correct for local variations of the detector response and ϕ_i their azimuthal position. Due to the experimental resolution in the approximation as in Eq. 4.2, a correction factor R needs to be applied to the observable of the elliptic flow $v_2 = \langle \cos[n(\phi - \Psi_2)] \rangle$. This correction factor was obtained from data using the "sub-events" technique [6], dividing an event in two subevents, one considering the positive (P) and one the negative (N) η-side yielding $R(\sum E_T) = \sqrt{\langle \cos[2(\Psi_2^N - \Psi_2^P)] \rangle}$.

4.1 Results

The resolution-corrected v_2 is calculated in intervals of p_T and η. While the η-dependence was found to be vanishingly weak [7], the p_T-spectrum exhibits a characteristic distribution as shown in Fig. 2. Up to around 3 GeV a rapid rise is visible followed by a decrease up to 8 GeV. From around 10 to 20 GeV, the p_T-dependence is rather weak. The strongest flow is observed in the mid-centrality intervals (30−40 % and 40−50 %). Higher order harmonics from v_2 to v_6 were measured based as well on the event plane method, the details can be found in Ref. [9]. A result of this analysis is shown in Fig. 3. The p_T-dependence is similar for all measured flow harmonics. One can note from that figure that v_2 does not give the highest contribution for most central collisions (0−5 %).

5. Conclusions

Two correlations measurements by ATLAS were highlighted, one using proton-proton collisions [3, 4], the other lead-lead collisions [7, 8, 9]. The pp analysis used a data-driven method to measure particle correlations which allows a direct comparison to predictions of several MC models as PYTHIA6, PYTHIA8 and PHOJET. It is observed that the complex structure is reproduced in MC, but not the strength of the correlation as observed in data. The results of the heavy ion analysis test hydrodynamic models in LHC regime by measurements of elliptic flow, which for the first time is measured in a broad range in η ($|\eta| < 2.5$) and p_T (0.5 to 20 GeV). More constraints are provided by measurements of higher harmonics up to v6 of angular anisotropy.

References

[1] M. Gyulassy and L. McLerran. New Forms of QCD Matter Discovered at RHIC. *Nucl. Phys. A*, 750, 30 (2005), arXiv:nucl-th/0405013, 2004.

[2] The ATLAS Collaboration. The ATLAS Experiment at the CERN Large Hadron Collider. *JINST*, 3 S08003, August 2008.

[3] The ATLAS Collaboration. Measurement of Inclusive Two-Particle Angular Correlations in Proton-Proton Collisions at $\sqrt{s} =$ 900 GeV and 7 TeV. ATLAS-CONF-2011-055, April 2011.

[4] The ATLAS Collaboration. Measurement of Inclusive Two-Particle Angular Correlations in pp Collisions with the ATLAS Detector at the LHC. To be subm. to *JHEP*, 2012.

[5] J. W. Monk and C. Oropeza-Barrera. The HBOM Method for Unfolding Detector Effects. *Subm. to Nucl. Instr. Meth.*, arXiv:1111.4896, January 2012.

[6] S. A. Voloshin, A. M. Poskanzer, and R. Snellings. Collective phenomena in non-central nuclear collisions. arXiv:0809.2949, Oct. 2008.

[7] The ATLAS Collaboration. Measurement of the pseudorapidity and transverse momentum dependence of the elliptic flow of charged particles in lead−lead collisions at $\sqrt{s_{NN}} =$ 2.76 TeV with the ATLAS detector. *Phys. Lett. B*, 707, 3−4, February 2012.

[8] The ATLAS Collaboration. Measurement of elliptic flow and higher-order flow coefficients with the ATLAS detector in $\sqrt{s_{NN}} =$ 2.76 TeV TeV Pb+Pb collisions. ATLAS-CONF-2011-074, May 2011.

[9] The ATLAS Collaboration. Measurement of the azimuthal anisotropy for charged particle production in $\sqrt{s_{NN}} =$ 2.76 TeV lead−lead collisions with the ATLAS detector. To be subm. to *Phys. Rev. C*, 2012.

PoS(WPCF2011)022